

17. *Pyroclastic Deposits distributed on the East Foot of Volcano Myôkô.*

By Isamu MURAI,

Earthquake Research Institute.

(Read Feb. 23, 1960.—Received March 31, 1960.)

Introduction

Volcano Myôkô is situated in the southern part of Niigata Prefecture, in Central Japan. There is no historic record of its eruptive activity. It is a double volcano consisting of a large central dome and a somma. Fumaroles and hot springs are found on the foot of the central dome. The eastern rim of the somma is eroded deeply by a barranco. A thick bed of pyroclastic deposits occupies the barranco and spreads out extensively at the east foot of the somma, forming a vast flat plane. The writer has studied these pyroclastic deposits and obtained several new data on the nature and the origin of them, which are presented in this paper with the results of the mechanical analyses of the deposits.

The writer wishes to express his great gratitude to Professor Hiro-michi Tsuya of the Earthquake Research Institute, Tokyo Univ., for his invaluable advice and encouragement. He is indebted to Mr. Ichirô Uehara of the Myôkô Sightseeing and Development Co. Ltd., and the employees of the Sekiyama Sport Hotel, for giving many facilities to his field study. He is also indebted to Mr. Yoshichi Hosoya of the Komoro Branch of the Earthquake Research Institute, for his aid in carrying out the mechanical analyses as well as for preparation of figures in this paper.

General Structure of the Volcano

Volcano Myôkô was constructed on a foundation of Tertiary formations, which are distributed on the floor of the barranco and develop on the north-east foot of the somma. The somma is composed mainly of repeated layers of lava flows of two-pyroxene-andesite. The uppermost layers of the somma consist of lava flows of olivine-bearing two-pyroxene-andesite and hornblende-pyroxene-andesite. The central lava dome, con-

sisting of quartz-olivine-bearing augite-hypersthene-andesite, develops in the caldera, the major and the minor diameter of which are 2.7 km from north to south and 2 km from east to west respectively. The eastern part of the central dome is partly destroyed, perhaps by a side-explosion. The eastern and the southern rim of the caldera are cut by barrancos, forming the deep valleys of Kita-jigoku-dani and Ôtagiri-gawa, and Minami-jigoku-dani and Shirotagiri-gawa respectively (Fig. 5). A thick bed of pyroclastic deposits dealt with in this paper develops in the eastern barranco and on the eastern skirt of the somma. The latest lava flow of hornblende-augite-hypersthene-olivine-andesite effused from the foot of the central dome and flowed into the eastern barranco.

Pyroclastic Deposits distributed on the East Foot of the Volcano

On the foot of the central dome and in the eastern barranco a thick bed of pyroclastic deposits, composed of porous lava blocks of hornblende-hypersthene-andesite and their fragments, is found under the latest lava flow of the central dome. The same bed is also distributed extensively on the east foot of the volcano, overlying the lava flows of the somma and the foundation of Tertiary formations (Fig. 1). The eastern border of its distribution lies along the course of the Seki-gawa. The flat surface of the deposits is dissected by U-shaped valleys, on the walls of which the vertical sections of the bed are exposed (Figs. 6, 7 and 8). The thickness of the bed is 50 m or more, and the area of its distribution is about 23 km². So the volume of the deposits is calculated at about 1.2 km³. There is no remarkable stratification in the bed, although layering of large blocks is sometimes found in the middle and upper parts. An ash layer of about 1 m thickness is found in the upper part of the bed in the vicinity of the central dome (Fig. 9). Natural charcoal is contained in the pyroclastic deposits, showing that these pyroclastic materials were very hot when they were deposited (Fig. 10). The lava blocks in the deposits are fairly porous, and their density is within a range of 1.2 to 1.9 (1.6 on the average). The matrix of the deposits consists of lava fragments, mineral grains (mainly plagioclase, hornblende and hypersthene) and glass fragments.

The pyroclastic deposits concerned here have been formerly considered as mud-flow deposits caused by collapse of the eastern part of the central dome¹⁾. They are more or less similar in features to mud-flow

1) N. YAMAZAKI, *Report, Earthq. Inv. Comm.* 8 (1896), 48-49. (in Japanese).

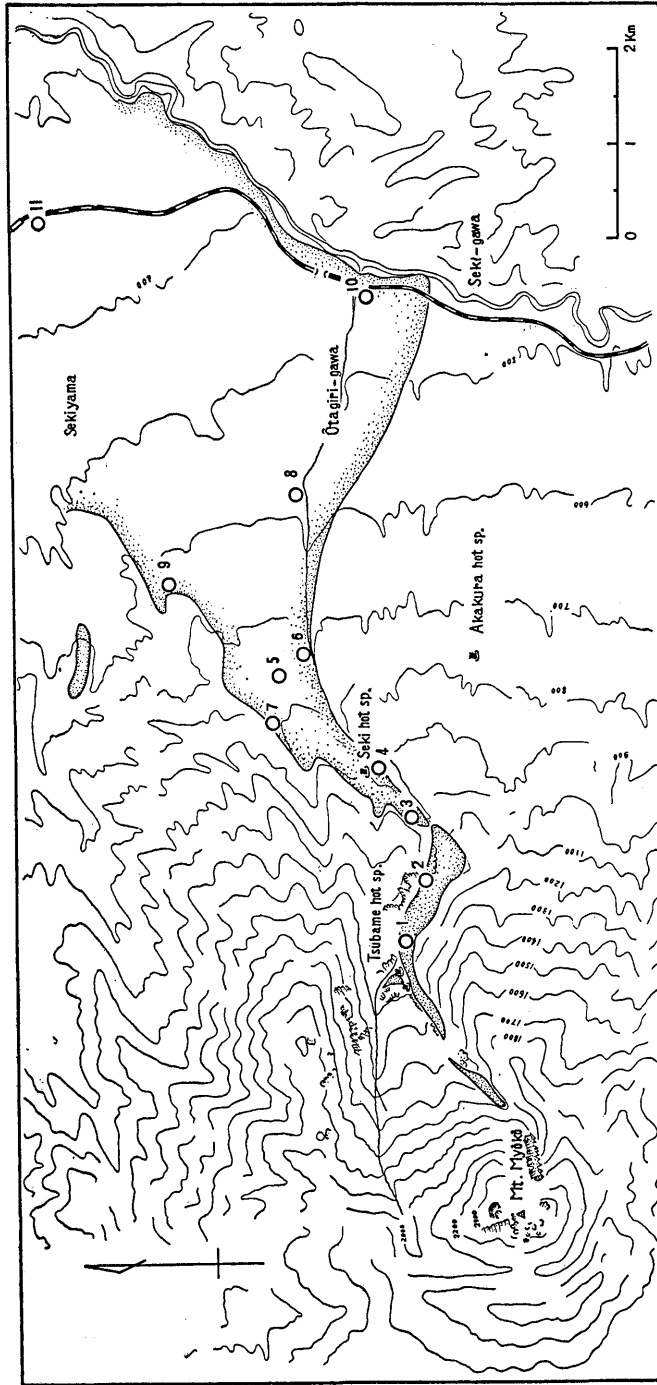


Fig. 1. Map of the eastern part of Volcano Myôkô, showing the distribution of the pyroclastic deposits and the localities of specimens collected for mechanical analyses.

deposits. The large blocks in them are somewhat angular and have faceted surface, suggesting that they were brought by disruption of solid rock mass. The constituents of the deposits are petrologically similar to the central lava dome. In spite of these characteristics, the volume of the deposits is too huge to be explained as the products of mud-flows caused by the collapse of the eastern part of the central dome. The volume of the collapsed mass of the central dome is only about 0.03 km³, while the volume of the deposits is about 30 times larger, and almost equal to the whole mass of the central dome. It is impossible to infer that these deposits were resulted only by disruption of a small part of the dome. S. Aramaki mentioned these deposits as an example of the pyroclastic flows of intermediate type in his classification (1957)²⁾. The writer considers that they may have been caused by explosive eruptions of the central dome followed by discharge of a large quantity of porous fragmentary materials, perhaps in a state of pyroclastic flow. Eruptions may have occurred several times, as may be inferred from the sedimentary features in the bed of the deposits such as layering of large blocks. The details of the course of eruptions have never been clarified. Careful studies on the structure and petrology of the central dome, as well as on the relationship between the dome and the deposits, may be necessary in order to explain exhaustively the origin and mechanism of accumulation of the pyroclastic deposits concerned.

Mechanical Analyses of the Pyroclastic Deposits.

The writer collected several specimens of the pyroclastic deposits in various localities, and carried out mechanical analyses of the specimens (Figs. 11 and 12). Localities where the specimens were collected are shown in Fig. 1. Specimens of 1 to 2 kg weight were collected for mechanical analyses. Mechanical analyses were carried out by means of sieving, decantation and pipette methods. Besides, all the results obtained by such laboratory work were corrected for the coarser fractions by referring to the photographs of the outcrops from which the specimens were picked up. Detailed description of such steps of the mechanical analyses will be omitted here. The final results of the mechanical analyses are shown in Table 1, each figure listed in the column represents the weight per cent of each fraction sized out by the mechanical analyses. Fig. 2 and Fig. 3 show the particle size distribution of the specimens by cumulative curves and histograms respectively. The diameters of

2) S. ARAMAKI, *Bull. Volcanol.*, [ii], **1** (1957), 53-54, (in Japanese).

Table 1. The results of the mechanical analyses.

ϕ \sp. no.	1	2	3	4	5	6	7	8	9	10	11
~-10	1.1		1.0								
-10~-9	2.2	1.5	2.2		0.6					1.7	
-9~-8	2.6	2.5	3.9	2.0	1.8		2.0	0.8		2.3	
-8~-7	2.8	3.2	2.7	3.0	2.9	1.8	3.0	2.5	1.5	3.1	3.5
-7~-6	4.2	4.0	4.4	4.1	4.0	3.4	5.5	3.9	3.0	3.7	4.0
-6~-5	5.3	6.2	6.3	4.2	6.5	3.6	7.1	5.0	4.1	3.7	4.5
-5~-4	6.6	6.3	8.1	4.8	8.5	3.9	6.3	5.1	4.6	4.0	5.5
-4~-3	4.8	5.2	7.4	4.9	8.0	6.0	4.2	4.7	5.9	3.3	6.0
-3~-2	2.9	4.8	6.7	5.0	6.0	10.0	3.9	4.5	6.9	4.1	6.5
-2~-1	4.4	5.1	7.0	5.8	5.5	10.1	4.7	4.9	7.0	5.1	6.7
-1~0	9.6	7.8	8.8	8.6	6.4	9.1	8.0	8.8	10.5	9.2	10.2
0~1	13.5	12.6	9.8	12.0	11.8	13.1	12.9	12.5	13.5	13.7	12.1
1~2	12.8	11.5	8.7	12.9	11.2	11.0	12.6	10.8	13.0	13.4	12.2
2~3	10.0	9.5	7.0	11.9	5.5	9.5	10.0	9.3	10.4	10.0	10.9
3~4	6.9	7.4	5.3	9.3	7.3	6.9	7.9	7.9	8.2	8.4	7.2
4~5	4.5	5.4	4.4	6.8	5.0	5.2	5.2	6.8	5.4	6.5	4.9
5~6	2.1	3.2	2.6	2.8	2.2	2.7	2.6	5.3	2.5	3.3	1.8
6~7	1.7	2.1	0.8	0.7	1.4	1.6	1.9	3.4	1.3	2.0	1.4
7~8	1.0	0.9	0.7	0.5	0.4	0.9	1.1	1.1	1.2	1.1	1.0
8~9	0.6	0.3	0.9	0.6	0.4	1.0	0.8	0.8	0.7	0.6	0.9
9~	0.4	0.5	0.3	0.1	0.6	0.2	0.3	1.9	0.3	0.8	0.7

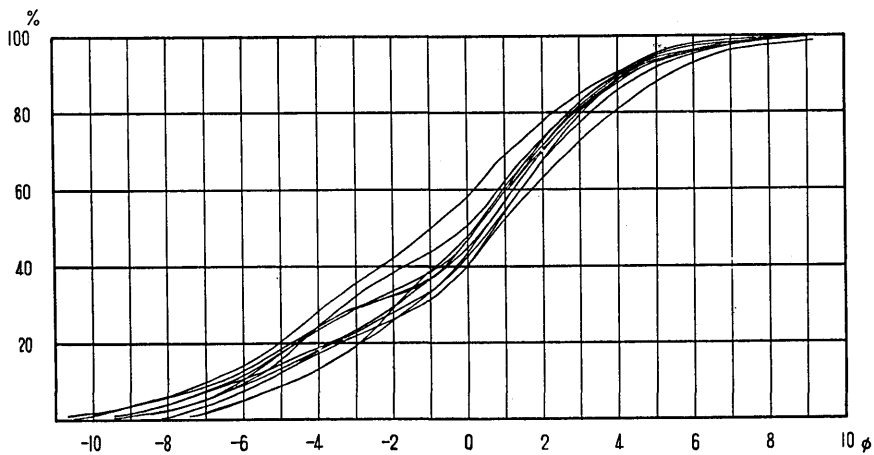


Fig. 2. Cumulative curves of particle size distribution.

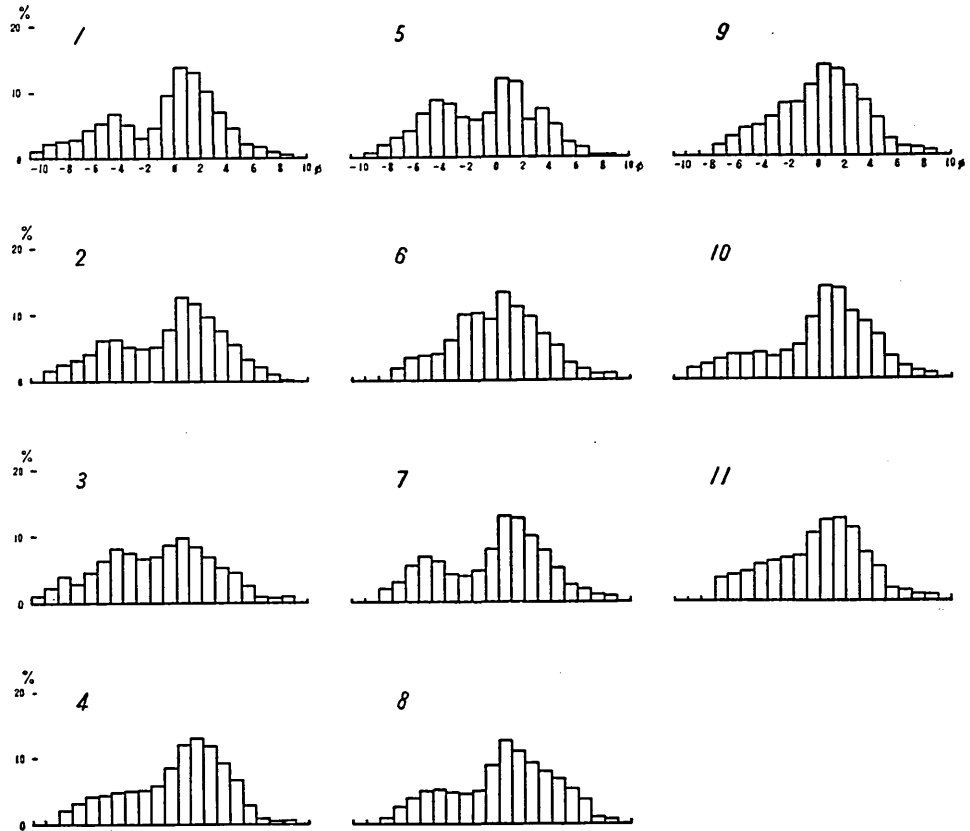


Fig. 3. Histograms of particle size distribution. The number of specimen is noted on the left of each histogram.

Table 2. Data on parameters of particle size distribution.

Specimen no.	Md_ϕ	M_ϕ	Q'	Q''	σ_ϕ	α_ϕ	$\alpha_{2\phi}$	β_ϕ	Remark
1	0.28	-1.05	3.07	-0.76	4.27	-0.31	-0.41	0.60	middle part
2	0.28	-0.85	2.59	-0.36	4.32	-0.26	-0.32	0.54	"
3	-0.98	-1.39	3.03	-0.28	4.24	-0.10	-0.16	0.59	upper part
4	0.63	-0.43	2.61	-0.47	3.96	-0.27	-0.42	0.51	lower part
5	-0.03	-0.92	3.05	-0.56	4.06	-0.22	-0.25	0.49	uppermost part
6	0.14	-0.05	2.30	-0.15	3.36	-0.06	-0.13	0.95	lower part
7	0.47	-0.89	3.09	-0.74	4.31	-0.32	-0.28	0.46	middle part
8	0.78	0.24	2.79	-0.21	4.35	-0.12	-0.17	0.51	upper part
9	0.47	-0.05	2.30	-0.27	3.45	-0.15	-0.22	0.63	uppermost part
10	0.74	-0.42	2.47	-0.39	4.18	-0.28	-0.39	0.62	middle part
11	0.28	-0.54	2.53	-0.42	3.76	-0.22	-0.37	0.59	uppermost part

particles in millimeters ξ are replaced here by ϕ as expressed $\phi = -\log_2 \xi$ for convenience. The phi values of the percentiles ϕ_5 , ϕ_{16} , ϕ_{25} , ϕ_{50} , ϕ_{75} , ϕ_{84} , and ϕ_{95} were read on the cumulative curves, and the approximate

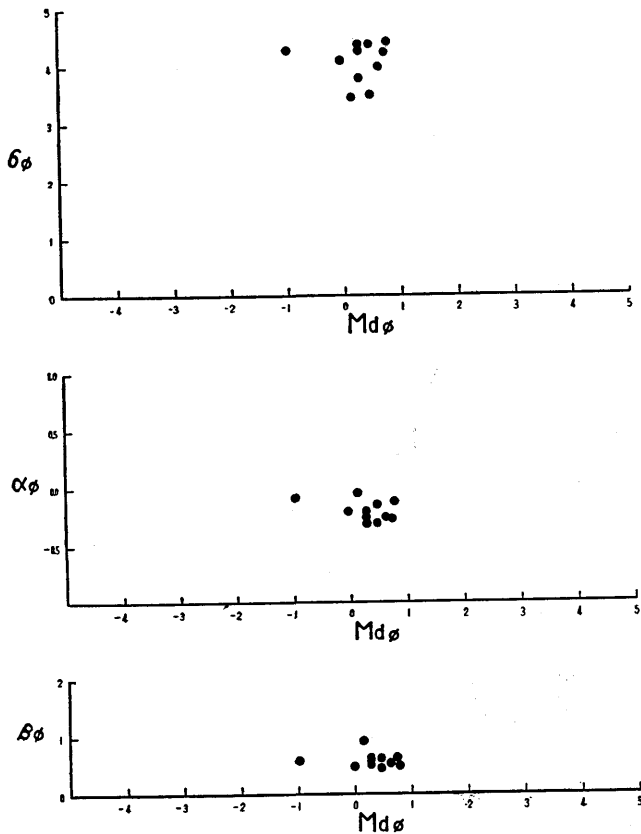


Fig. 4. The relation of the values of σ_ϕ , α_ϕ and β_ϕ to the values of Md_ϕ .

values of every sort of parameter of the particle size distribution were calculated from the following relations. The values of these parameters are listed in Table 2.

$$\begin{aligned}
 Md_\phi &= \phi_{50}, & M_\phi &= (\phi_{16} + \phi_{84})/2, \\
 Q' &= |\phi_{75} - \phi_{25}|/2, & Q'' &= (\phi_{75} + \phi_{25} - 2\phi_{50})/Q', \\
 \sigma_\phi &= |\phi_{84} - \phi_{16}|/2, & \alpha_\phi &= (M_\phi - \phi_{50})/\sigma_\phi, \\
 \alpha_{2\phi} &= \frac{(\phi_5 + \phi_{95})/2 - \phi_{50}}{\sigma_\phi}, & \beta &= \frac{(\phi_{95} - \phi_5)/2 - \sigma_\phi}{\sigma_\phi}.
 \end{aligned}$$

Md_ϕ , Q' and Q'' are median, deviation and skewness respectively, obtained by the quartile method, while M_ϕ , σ_ϕ , α_ϕ and $\alpha_{2\phi}$, and β_ϕ are

mean, deviation, skewness and kurtosis of the Inman's phi measure system³⁾.

The results of the mechanical analyses of 11 specimens of the pyroclastic deposits are summarized as follows:

1) The size characteristics of all specimens are similar to each other, in spite of the fact that specimens were collected from the different horizons of the bed in various localities. Systematic variation of coarseness with distance from the source could not be found. The values of median diameters Md_ϕ stay exclusively in a range of -1.0 to 0.8 in ϕ scale, and the mode of the size distribution always lies in the fractions of 0 to 2 . Tailing-out of both the coarser and finer fractions are found in every specimen, and a sub-mode may be sometimes found in the tailing-out part of the coarser fractions, lying in the size of -6 to -4 .

2) The sorting is fairly bad, as the values of Q' are in a range of 2.3 to 3.1 , and the values of σ_ϕ are in a range of 3.3 to 4.4 . These values are somewhat larger than those of the pumice-flow deposits. The values of α_ϕ , which represent the degree of skewness, stay in a negative range of -0.3 to 0 . The values of β_ϕ , the parameter of kurtosis, are in a range of 0.4 to 1.0 . The shape of the particle size distribution of every specimen is considerably flat as to be seen on the histogram.

3) The size characteristics of the pyroclastic deposits concerned are somewhat similar to these of the *nuée ardente* deposits, for example the *nuée ardente* deposits of the central cone of Volcano Hakone. They also show a little resemblance to these of mud-flow deposits, for example the mud-flow deposits of Volcano Komagatake and Volcano Bandai. The shape of particle size distribution is rather stable, and the values of parameters stay exclusively in narrow ranges as shown in Table 2 and Fig. 4, in the same way as in the case of pumice-flow deposits. This seems to be dissimilar to the case of mud-flow deposits in which matters may be otherwise.

Summary

It seems apparent that the pyroclastic deposits which are distributed on the east foot of Volcano Myôkô are not the products of mud-flows caused by disruption of the eastern part of the central dome, as they have been hitherto considered. They may have been the result of the explosive eruptions of the central dome followed by discharge of a large quantity of porous fragmentary materials, descending down the moun-

3) D. I. INMAN, "Measures of describing the Size Distribution of Sediments", Jour. Sed. Petrol., **22** (1952), 125-145.



Fig. 5. The central dome and the somma of Volcano Myōkō, looking from loc. no. 6 in the valley of the Ottagiri-gawa.

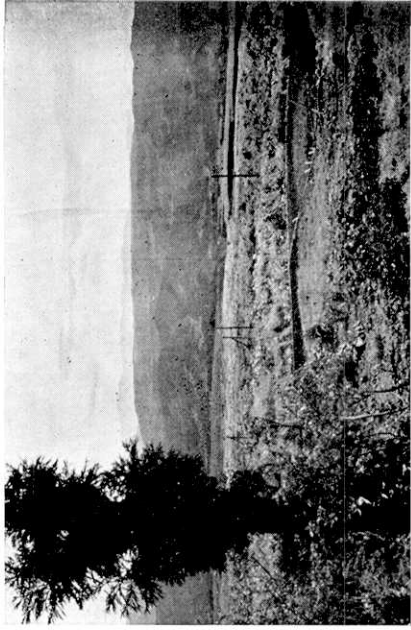


Fig. 7. The surface of the pyroclastic deposits, near loc. no. 5.

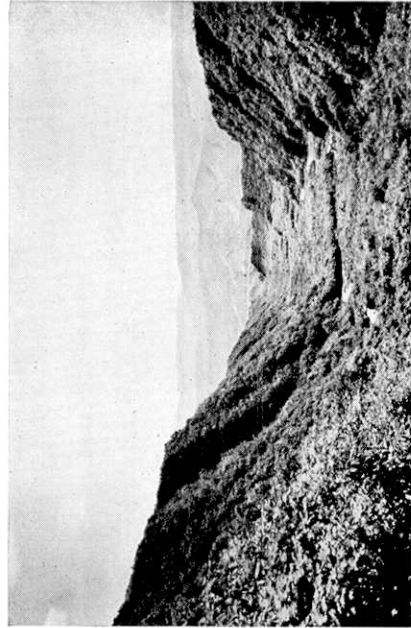


Fig. 6. U-shaped valley of the Ottagiri-gawa cutting into the pyroclastic deposits, looking from the upper side, near loc. no. 6.

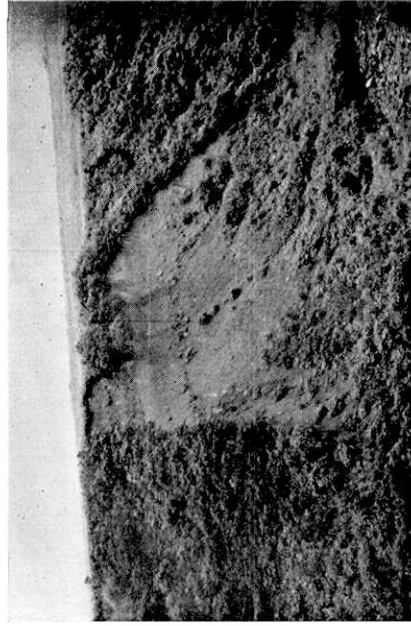


Fig. 8. The vertical section of the pyroclastic deposits exposed on the valley-wall of the Ottagiri-gawa, near loc. no. 8.



Fig. 11. The outcrop of the pyroclastic deposits from which specimen no. 1 was collected.



Fig. 12. The outcrop of the pyroclastic deposits from which specimen no. 10 was collected.



Fig. 9. Ash layer embedded in the pyroclastic deposits, near Tsubame hot spring.



Fig. 10. Natural charcoal buried in the pyroclastic deposits, near Tsubame hot spring.

tain-slope in a state of pyroclastic flow. Further studies on the pyroclastic deposits as well as on the central dome are necessary in order to clarify the origin and mechanism of deposition of the pyroclastics.

17. 妙高火山東麓に分布する火砕堆積物

地震研究所 村 井 勇

妙高火山は新潟県南部に位置する火山で、噴火の記録はない。二重火山で、外輪山は主として複輝石安山岩の熔岩よりなる。南北 2.7 km, 東西 2 km の大きさを持つカルデラの中には、普通輝石・紫蘇輝石・角閃石・安山岩の熔岩円頂丘が大きく成長している。外輪山の東壁は火口瀬によつて深く刻まれているが、この火口瀬の内部に火山砕屑物質よりなる堆積物が厚い層をなして分布している。この堆積物は、中央円頂丘の麓では、最後に噴出した角閃石・橄欖石・安山岩の熔岩によつておおわれている。外輪山の東麓では非常に広い範囲にわたつて分布しており、その先端は中央円頂丘より約 10 km はなれた関川にまで達している。分布面積は約 23 km² におよび、層厚は 50 m またはそれ以上と見られるから、この火砕堆積物の総体積は約 1.2 km³ と計算される。

この堆積物は角礫と細粒物質の混合したもので、一見したところ火山泥流の堆積物のように見受けられる。角礫はほとんどすべて多孔質のガラス質石基を持つた角閃石・紫蘇輝石・安山岩の破片で、細粒物質は斜長石・角閃石・紫蘇輝石等の鉱物粒およびガラス破片よりなり、粘土鉱物はほとんど含まれない。その厚い層全体が均質で、なんら特別な構造を示さないが、角礫を多く含む層が部分的に見られる場合がある。中央円頂丘の付近では上部に厚さ 1 m ほどの火山灰層が挟まれている。また、天然木炭を含んでおり、堆積当時から高温であつたと見られる。

中央円頂丘の東側には爆裂火口状の地形が見られる。問題の火砕堆積物はこの部分の崩壊によつて発生した泥流の堆積物と従来考えられてきた。しかし崩壊部分の体積は約 0.03 km³ にすぎず、1.0 km³ 以上の体積を持つ堆積物の生因をこれで説明することは困難である。荒牧重雄はこの堆積物を中間型火砕流の例に加えている (1957 年)。中央円頂丘の構造やこの火砕堆積物との関係を詳しく調査した上でなくては確実な結論は得られないが、おそらく円頂丘の崩壊とともに火砕流が発生したものと見られ、このような噴火が繰返えされた結果火砕堆積物の厚層が東麓一帯に発達したと考えられる。

火砕堆積物の層から合計 11 個の試料を採集して機械分析を行なつたが、粒度分布はいずれもきわめてよく類似している。 Md_{ϕ} は -1.0 と 0.8 の範囲内にありよくそろつている。 σ_{ϕ} は 3.3~4.4 で、一般の軽石流堆積物の場合より大きい。モードは $\phi=0\sim 2$ の間に常に現われる。また $\phi=-6\sim -4$ の間に副モードが見られる場合が多い。 α_{ϕ} は常に負の値をとる。 β_{ϕ} は 0.4~1.0 で、粒度分布の形が平らであることを示している。このような粒度分布の特徴は火砕流堆積物に共通に見られるものであるが、また泥流堆積物の場合とも類似の点をもっている。ただし、泥流堆積物では粒度分布の形の変化が大きく、パラメーターの値がよくそろわないのが普通のものである。